COMPOUND-LENS INJECTOR FOR A 19-MeV, 700-kA ELECTRON BEAM*

T. W. L. Sanford, J. W. Poukey, J. A. Halbleib, and R. C. Mock†
Sandia National Laboratories
P. O. Box 5800, Albuquerque, NM 87185-5800 USA

Abstract

A robust injector capable of controlling the radius and angle of incidence of the intense, pulsed, annular electron beam extracted from the HERMES-III accelerator is described. The injector, called the compound lens, uses a tapered anode to control the beam electrostatically, followed by a gas cell with externally applied current to control the beam magnetically. Adjustment of the anode-cathode gap and external current of the injector permits the mean radius and injection angle of the beam to be defined independently of one another. Measurements of these quantities confirm model expectations.

I. INTRODUCTION

The extended planar-anode diode[1] with a thin anode window has been used to inject[2] a 25-ns, 19-MeV, 700-kA, annular electron beam into gas-filled drift cells for beam transport to bremsstrahlung targets located downstream of the HERMES-III accelerator.[3] By adjusting the anode-cathode (AK) gap of the diode, the radius and angle of incidence of the annular beam at injection can be varied. Increasing the AK gap increases the radius and simultaneously decreases the angle. This adjustment enables injection angles as low as ~20° (zero degrees being parallel to the beam propagation direction) to be achieved before significant beam is lost to the side wall upstream of injection. This restriction in injection angle limits the subsequent transport efficiency achievable in a downstream drift cell.[2]

By using the compound-lens diode as an injector,[4] this limitation is removed. This diode was developed to improve the uniformity of the radiation[5] generated by HERMES III, which was designed to produce an intense burst of bremsstrahlung for the study of radiation effects induced by γ rays.[3] In this diode, the beam is accelerated to a thin, conical anode window separating the vacuum AK gap from a gas-filled lens (Fig. 1). As in the extended planar-anode diode, increasing the AK gap increases the radius and simultaneously decreases the angle of the annular beam at the anode. After passage through the window, the beam is rapidly charge and effectively current neutralized by the 3 Torr of N_2 gas contained within the lens. With no applied external current, the beam propagates nearly ballistically in the lens, owing to the radial distribution of the net-current density.[6] However, application of an external current I_E produces an azimuthal magnetic field that enables a given angle of incidence at the exit of the lens to be achieved independently of the incident radius.

In this paper, we theoretically model and experimentally characterize the electron flow in the compound-lens diode when it is used as a bremsstrahlung source (Fig. 1).[5] Results when it is used as an injector for a short drift cell with a 20-cm AK gap are given in Ref. 7. Here we emphasize results obtained as the AK gap is increased to 40 cm. The model combines the MAGIC code[8] to simulate the time-dependent electron flow in the AK gap and lens with the CYLTRAN code of the ITS system[9,10] to model window effects and the subsequent transport in the target. MAGIC is a two-dimensional, time-dependent, electromagnetic, particle-in-cell code. CYLTRAN is a two-dimensional, time-independent, Monte-Carlo electron-photon, transport code. The model is similar to that described in Ref. 1. It uses the voltage pulse measured at the diode as input to MAGIC. MAGIC then generates the time-dependent space-angle distribution of the electron beam at the lens. This distribution is time integrated and, along with an experimental electron kinetic-energy distribution, is used as input to CYLTRAN.

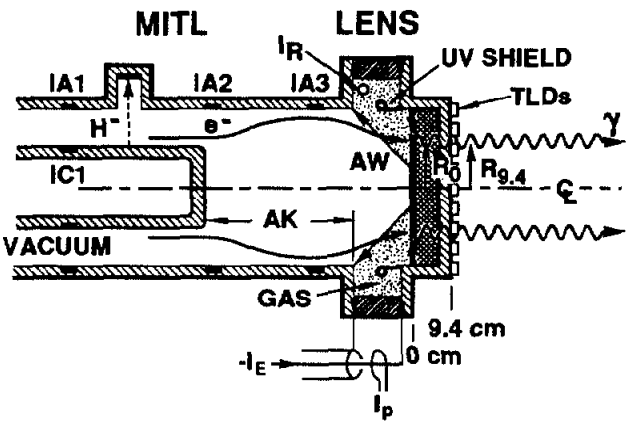

Figure 1. Schematic of compound-lens diode.

Section II describes the experimental arrangement, including some details of the diode. Section III describes the operation of the diode and presents some model results and comparisons. Section IV summarizes our conclusions.

II. EXPERIMENTAL ARRANGEMENT

The general arrangement, operating conditions, and diagnostics are those discussed in Refs. 1, 2, and 5. Briefly, current shunts in the anode (IA1) and cathode (IC1), as shown in Fig. 1, measure the incident current and permit the voltage pulse to be estimated from parapotential flow theory.[11] For a 20-cm AK gap, the time dependence of voltage, current, beam radius, and output beam angle are given in Fig. 3 of Ref. 7. The peak voltage is corroborated within 4% by simultaneously measuring the range of H^- ions[12] for selected shots. For the data presented here the peak voltage was measured to be 19.0±0.5 MV, where the uncertainty corresponds to shot-to-shot variation. This value is identical to that measured previously under nominal operating conditions.[13]

*This work was performed under U.S. Dept. of Energy Contract No. DE-AC04-76DP00789.
†Ktech Corp., Albuquerque, NM

0-7803-1203-1/93$03.00 © 1993 IEEE

The N_2 gas within the lens is contained by two 0.3-mm thick Ti windows welded at a 5-cm radius, and held apart at a 52-cm radius by a Lucite insulator 28-cm long (Fig. 1). The gas is held at pressures between 3 and 10 Torr to facilitate rapid charge and current neutralization of the incident beam. Below an I_B of 160 kA, the lens is operated at 3 Torr—the pressure that optimizes the neutralization (≥ 96%) of the beam current.[6] Above 160 kA, to prevent breakdown across the insulator from the higher inductive voltage drop, we operate the lens at 10 Torr. This higher pressure is within the capability of the windows to contain the gas without significant distortion—20 Torr is the estimated maximum. The calculated multiple-Coulomb-scattering produced by the two windows results in a beam divergence of about ±6°. This divergence is similar in magnitude to the intrinsic dispersion (±4°) about the mean angle of incidence at the anode (to be discussed in the next section). The energy loss through the windows is calculated to be 0.45 MeV.

An optimized bremsstrahlung target was placed immediately downstream of the lens (Fig. 1). Measurements of the annular radiation pattern from images taken with the X-ray pinhole camera enabled the time-integrated radial impact position $\mathbf{R_0}$ of the annular beam at the exit (z=0 cm) of the lens to be estimated. Combining $\mathbf{R_0}$ with measurement of the radius of the peak off-axis radiation dose $\mathbf{R_{9.4}}$ obtained from TLDs (thermoluminescent dosimeters) at the downstream face (z=9.4 cm) of the target permits the angle of incidence θ_0 of the time-integrated beam to be determined ($\theta_0 = \tan^{-1}[(\mathbf{R_0}-\mathbf{R_{9.4}})/9.4]$).

III. DIODE OPERATION AND MODEL RESULTS

The compound-lens diode provides a matched load to the upstream magnetically-insulated transmission line[3] of HERMES III for the 20- to 40-cm AK gaps considered here. The MAGIC simulations indicate that once an electron sheath forms above the cathode for these AK gaps, the sheath, together with the flow near the tip of the cathode, leads to a well-defined annulus of beam electrons that moves towards the lens. As the voltage and associated current ramp up at the tapered anode window (aw), the radius R_{aw} of this annular ring sweeps radially inward, attains a minimum radius near the time of peak voltage, and then sweeps radially outward as the voltage ramps down.[7] The sweeping is due to the shorting of the repulsive radial electric field at the anode window and the continued presence of the pinching self-magnetic field, which increases or decreases with beam current.

Early and late in the voltage pulse, the low-energy electrons are lost to the side anode wall, or are swept into the insulator (when a finite I_E is flowing in the lens). These combined losses are small for our parameters.[7] Once the energy of the electrons exceeds 3 MeV, the electrons are injected forward. Comparison of the forward current pulse with the voltage pulse also shows that, after the voltage exceeds about 9 MV, the voltage and current pulses have nearly the same shape. Thus, over this range the diode impedance is almost constant.

Figures 2A and 2B show the corresponding simulated radial and angular distribution of the beam at the anode window at peak voltage. Figure 2 is the result for an AK gap of 40 cm and $I_E = 90$ kA. Figure 2A indicates the presence of the dominant annular beam, showing that R_{aw} equals 19 cm and has a full-width at half-maximum of about 8 cm. The electrons at smaller radii originate from the cathode front face. As the radial impact position of the electrons increases at the anode window, more beam current is enclosed within that radius, and the self-magnetic pinching force increases. Because the repulsive radial electric field (which prevents the beam from pinching far upstream of the anode window) is shorted at the anode, the angle of incidence θ_{aw} thus increases with increasing radius (Fig. 2B). At R_{aw}=19 cm, the associated angle of incidence θ_{aw} is 15.4°.

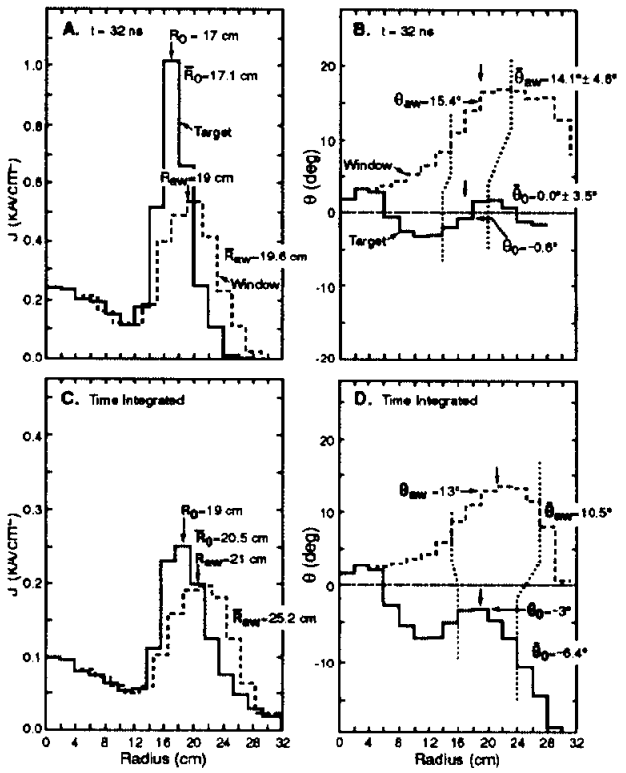

Figure 2. (A) Simulated electron beam radial current-density profiles and (B) associated angular distributions at the anode window [aw] (dashed lines) and lens exit [z=0 cm] (solid lines) at peak voltage. Corresponding (C) electron beam radial current density profiles and (D) associated angular distributions at the anode window and lens exit, time-integrated over the voltage pulse. Configuration is that of Fig. 1 with AK=40 cm and I_E=90 kA. The dotted lines in (B) and (C) indicate the radii corresponding to the full-width at half-maximum of the radial beam distributions of (A) and (C), respectively. Notation: radial averages indicated by bars over the symbol; time averages by bold face.

For times earlier or later than that corresponding to the time of peak voltage (32 ns), the radial impact position R_{aw} is increased, and the associated pinch angle θ_{aw} is reduced, owing to the reduced magnetic pinching from the lower beam current. Thus, the time-integrated radial (Fig. 2C) and angular (Fig. 2D) distributions at the anode window are modified relative to those shown at peak power. Specifically, because of the larger radii and smaller pinch angles at lower voltage, the radial distribution is skewed toward larger radii and the angular distribution is skewed toward smaller angles, especially at large radii. Both distributions retain, however, the main characteristics calculated

at peak voltage, because the bulk of the beam occurs near those conditions. For the 40-cm AK-gap case, the radius $\mathbf{R}_{aw}$ of the time-integrated annular beam is 21 cm (Fig. 2C), which is an increase of only 2 cm over that calculated at peak voltage. The associated angle θ_{aw} at $\mathbf{R}_{aw}$ is also close to the θ_{aw} of 15.4° calculated at peak voltage (Fig. 2D).

Because the repulsive radial electric force exceeds the pinching magnetic force far upstream from the anode window, as the AK gap is increased, the beam experiences a longer region over which it expands radially before being pinched due to the shorting of the radial electric field and the continued presence of the magnetic pinching field at the anode window. Accordingly, adjusting the AK gap permits the radius and the correlated angle at the anode window to be varied. Over the range of AK gaps from 20 to 40 cm, $\mathbf{R}_{aw}$ increases from 16 cm[7] to 21 cm (Fig. 2C) and the correlated θ_{aw} decreases from 17° to 13° (Fig. 2D).

When using a bremsstrahlung target to generate uniform radiation fields (Fig. 1), normal angles at the target are desired. By adjusting I_E, the associated external magnetic field (which turns the annular beam in the lens) is controlled, enabling the desired angle of incidence at the exit of the lens (z=0 cm) to be achieved independently of AK gap. Simulations show, for example, that for I_E=90 kA and AK = 40 cm, the time-integrated angle of incidence averaged over radius is reduced from $\bar{\theta}_{aw}$ = 10.5° at the entrance of the lens to $\bar{\theta}_0$ = -6.4° at the exit (Fig. 2D). At peak voltage, the corresponding angles are changed from θ_{aw} = 14.1°±4.6° at the entrance to θ_0 = 0.0°±3.5° at the exit (Fig. 2B). Thus the simulation predicts normal incidence for this case.

Figure 3 compares the simulated and measured time-averaged lens exit angle θ_0 of the beam at $\mathbf{R}_0$, for AK= 40 cm, as a function of I_E. The measured values systematically exceed the simulation values. The measured values are based on $\mathbf{R}_0$ and $\mathbf{R}_{0.4}$ (Fig. 1). $\mathbf{R}_0$ is derived from the radial profile on the film, where distortion leads to an overestimate by several cm.[7] A 1-cm shift in $\mathbf{R}_0$ leads to a 6° shift in θ_0. If this systematic error is combined in quadrature with the statistical measuring error (shown in Fig. 3), then the simulation point falls within the experimental uncertainty.

IV. SUMMARY

The predicted radial sweeping of the electron beam, leading to a well-defined annular beam at the entrance and exit of the lens, is confirmed by the measurements.[7] Adjustment of the AK gap over the range 20 to 40 cm causes the time-integrated radial impact position $\mathbf{R}_0$ at the exit to increase from 11 to 16 cm when no external current I_E is present. Over this range, the corresponding angle of incidence θ_0 decreases from about 17° to about 13°.

According to simulation and measurement, increasing I_E does not change $\mathbf{R}_0$ much. The major effect of adjusting I_E is to change the exit angle, independent of the incident radius, as in Fig. 3. For a 40-cm AK gap, for example, increasing I_E from 0 to 75 kA reduces θ_0 from 13° to 0°, and simultaneously increases $\mathbf{R}_0$ by only 3 cm. When the beam is incident on bremsstrahlung targets (Fig. 1) or injected into long drift cells, such angles are useful for producing uniform radiation fields and for efficient transport, respectively.

In conclusion, we have shown theoretically and experimentally on HERMES III that the compound lens provides an efficient method for controlling the radial and angular distributions of intense, pulsed, annular electron beams.

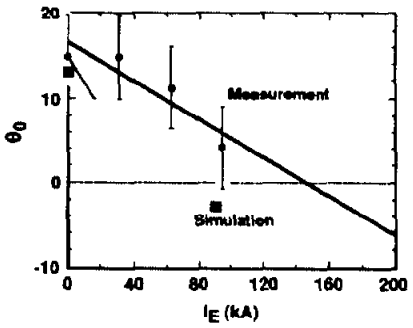

Figure 3. Comparison of measured estimate (●) and simulated (■) time-averaged lens-exit angle θ_0 at $\mathbf{R}_0$ as a function of I_E for geometry of Fig. 1, with AK=40 cm.

ACKNOWLEDGMENTS

We thank D. A. Muirhead and P. W. Spence (Pulse Sciences Inc.) for engineering support and useful discussions; W. H. McAtee, K. A. Mikkelson, V. Harper-Slaboszewicz, R. Westfall, and the HERMES-III crew for technical support; W. Beezhold, J. R. Lee, J. E. Maenchen, J. E. Powell, and J. J. Ramirez for vigorous programmatic support; and R. P. Kensek for reviewing the paper.

REFERENCES

[1] T. W. L. Sanford, Phys. Fluids **B3**, 2387 (1991) and references therein.

[2] T. W. L. Sanford, J. A. Halbleib, W. H. McAtee, K. A. Mikkelson, R. C. Mock, J. W. Poukey, D. R. Welch, J. Appl. Phys. **70**, 1778 (1991).

[3] J. J. Ramirez, K. R. Prestwich, and I. D. Smith, Proceedings of the IEEE, **80**, 946, (1992) and references therein.

[4] T. W. L. Sanford, J. A. Halbleib, J. W. Poukey, T. Sheridan, D. Muirhead, C. E. Yagow, K. A. Mikkelson, R. Mock, P. W. Spence, and H. Kishi, in *Digest of Technical Papers of 7th IEEE Pulsed Power Conference*, Monterey, CA. (IEEE, New York, 1989), pp. 441-444.

[5] T. W. L. Sanford, J. A. Halbleib, W. H. McAtee, K. A. Mikkelson, R. C. Mock, and J. W. Poukey, J. Appl. Phys. **69**, 7283 (1991).

[6] T. W. L. Sanford, J. W. Poukey, R. C. Mock, and D. R. Welch, J. Appl. Phys. **71**,472 (1992).

[7] T. W. L. Sanford, J. W. Poukey, J. A. Halbleib, and R. C. Mock, in press, J. Appl. Phys. **73**, (1993).

[8] T. D. Pointon, J. Comput. Phys. **96**, 143 (1991).

[9] J. A. Halbleib and T. A. Mehlhorn, Nucl. Sci. Eng., **92**, 338 (1986).

[10] J. A. Halbleib, *Monte Carlo Transport of Electrons and Photons*, edited by T. M. Jenkins, W. R. Nelson, and A. Rindi (Plenum, New York, 1088), pp. 249-284.

[11] J. M. Creedon, J. Appl. Phys. **46**, 2946 (1975); **48**, 1070 (1977).

[12] S. Lapin, G. W. Cooper, L. Davis, J. Bailey, W. A. Stygar, A. Carlson, and P. Reyes, Rev. Sci. Instrum. **63**, 4895 (1992).

[13] T. W. L. Sanford, J. A. Halbleib, L. J. Lorence, J. G. Kelly, P. J. Griffen, J. W. Poukey, W. H. McAtee, and R. C. Mock, Rev. Sci. Instrum. **63**, 4795 (1992).